Enhancing Exoskeleton Transparency with Motion Prediction: An Experimental Study

Alexandre Oliveira Souza, Jordane Grenier, François Charpillet, Serena Ivaldi, Pauline Maurice

Enhancing Exoskeleton Transparency with Motion Prediction: An Experimental Study

Alexandre Oliveira Souza[1, 2], Jordane Grenier[2], François Charpillet[1], Serena Ivaldi[1], Pauline Maurice[1]

***Abstract*—Controlling active exoskeletons for occupational assistance is a challenge. Unlike for rehabilitation exoskeletons, Electromyography (EMG) sensors can hardly be used for control in an industrial environment. The control of assistive exoskeletons needs to rely on onboard sensors to follow the human and assist when needed. This study explores the use of motion prediction, to enhance exoskeleton control in the absence of payloads. When no payloads are involved, the exoskeleton should be transparent meaning that the interaction forces between the exoskeleton and the user should be minimal. We conducted an experiment using a 3D-printed active elbow exoskeleton and compared exoskeleton control methodologies based on dynamic modeling and human motion prediction. Fifteen participants performed a repetitive pointing task under a baseline, two non-predictive controllers and two predictive controllers. The results demonstrated a significant reduction in interaction forces—up to 45%—with predictive controllers compared to non-predictive controllers. While motion prediction enhanced exoskeleton transparency, the force magnitude in this study was small, so users could hardly discern the improvement. Future research will investigate motion prediction for exoskeleton control in the context of load-handling assistance.**

I. Introduction

Occupational exoskeletons are a promising solution to help reduce work-related musculoskeletal disorders, owing to their potential to assist or augment the human user by providing additional torque when needed [1], [2]. They can be categorized into passive and active devices. Passive exoskeletons rely on springs or mechanical actuation to provide assistive torque to the user. They are designed for specific tasks (e.g., shoulder support in overhead work [3], lumbar support in forward bent postures [4]). However they lack versatility: they have been shown more useful for static work [5], and their high task-specificity is an obstacle to their long-term acceptance [6]. Conversely, active exoskeletons rely on controllable actuators, which allow for more versatility since assistive torques can be adapted to the context and the user's needs. However, providing appropriate and timely assistance remains a challenge [7]: when assistance is not needed, exoskeletons must be transparent for the user and the assistive torque must be given at the right time, when payloads must be carried, for example.

Lower-limb exoskeleton controllers generally leverage the cyclicity of locomotion (e.g., walking, running, stairs climbing) to generate phase-dependent torque profiles [8], [9]. Conversely, upper-limb movements are rarely cyclical, hence similar techniques cannot apply to upper-limb exoskeletons. A popular line of research uses electromyography (EMG), or even Electroencephalography (EEG), signals to detect the human's motion intention and adapt the upper-limb assistive torque accordingly [10]–[12] . But such approaches are largely limited to lab studies, due to the difficulty in using EMG data in real-life settings.

An alternative approach is to perform motion prediction based on kinematic data, ideally using only sensors embedded on the exoskeleton to limit invasiveness. Human motion prediction is an active field of research in various areas, such as pedestrian intention prediction [13] or human-robot collaboration [14]. Generative models [15], Recurrent Neural Networks [16] or Transformer-based diffusion models [17] have been

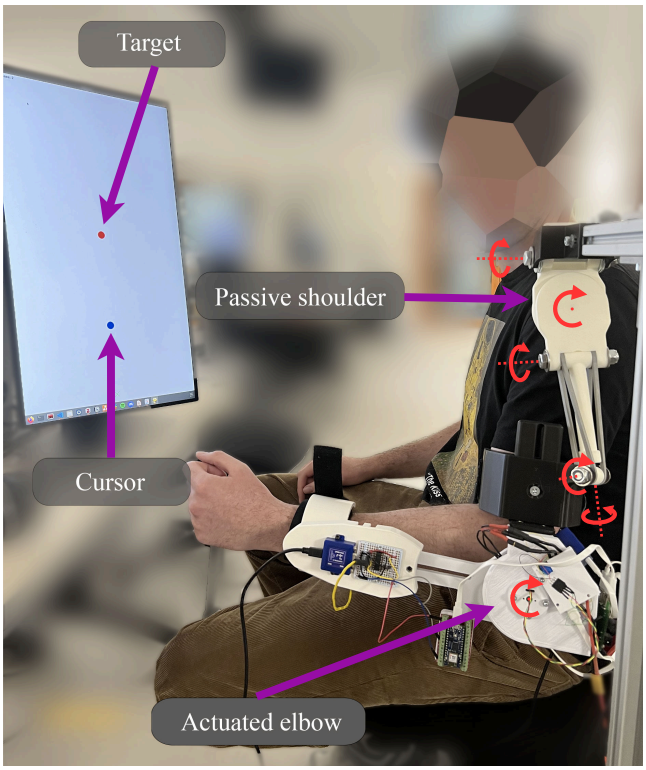

Fig. 1: Experimental setup: A participant performing the pointing task with the exoskeleton (the red arrows show the joint rotation directions, only the elbow is actuated, the other joints are passive). The movement of the cursor on the screen was controlled with the exoskeleton elbow flexion. Both predictive and non-predictive controllers were tested, in order to assess the effect of motion prediction on exoskeleton transparency.

[1] Université de Lorraine, CNRS, Inria, LORIA, F-54000 Nancy, France
[2] Safran Electronics & Defense, Valence, France

used to predict human intention. Simpler architectures such as Multi-Layer Perceptrons (MLP) have also shown comparable or better results with easier-to-train algorithms [18]. However, few studies have proposed to use kinematic-based motion prediction for upper-limb exoskeleton control. Jamsek *et al.* combined Probabilistic Movement Primitives with a flow controller for repetitive task assistance [19]. Lanotte *et al.* used adaptive Dynamic Motion Primitives to predict the user's hip motion in discrete movements with a hip assistance exoskeleton for load-carrying [20]. In a previous work, we introduced an LSTM-based motion prediction architecture for upper-limb exoskeleton control [21].

Motion prediction therefore seems a promising avenue to improve active exoskeleton control. For torque-controlled exoskeletons, it could help compensate for dynamic effects or uncertainties in the exoskeleton dynamic model, thereby enhancing the interaction with the user.

A crucial concept in human-exoskeleton interaction is *transparency* [22], defined as the ability to not apply any undesired force: when no assistance is needed, the human-exoskeleton interaction force should be minimal to avoid perturbing the human motion [23]. When working with a robotic manipulator, Jarrasse *et al.* showed that motion prediction could increase transparency [24]. But to the best of our knowledge, no study has evaluated the benefit of motion prediction on exoskeleton transparency.

This work investigates whether adding motion prediction in the control of an upper-limb exoskeleton affects transparency. We propose an MLP architecture to predict the arm motion of the user and exploit this prediction to compute the assistive torque of an elbow exoskeleton (Section II). In a pointing task user-study, we compare prediction-based controllers with standard gravity-compensation and dynamics-compensation controllers (Section III). Results show that prediction reduces human-exoskeleton interaction force, i.e. improves transparency, but does not noticeably improve the user's perception of the exoskeleton (Section IV).

II. Exoskeleton

A. Hardware Description

The exoskeleton used in this work is a 3D printed prototype upper-limb exoskeleton, with a 3 degrees of freedom (DoFs) passive shoulder joint and a 1 DoF actuated elbow joint (Fig. 1). It is attached to the user's arm and forearm with straps, but fixed to a supporting structure above the shoulder joint. The lengths of the exoskeleton arm and forearm are adjustable to fit different users. The exoskeleton weighs 1.01 kg, and the mass of the forearm part is 0.293 kg. Inertial parameters of the exoskeleton structure are calculated with the Solidworks CAD model, using the measured mass of each part and assuming a uniform mass distribution within each part.

The exoskeleton elbow is actuated with a direct-drive brushless motor of 200 W (rated torque of 1 N.m), controlled by an STM32-G431-Discovery ESC microcontroller[1]. An AS56 positional encoder measures the motor angular position (q_{enc}), from which the motor angular velocity ($\dot{q}_{enc}$) and acceleration ($\ddot{q}_{enc}$) are estimated with low-pass filtering and numerical derivation. Two LPMS-CU2 Inertial Measurement Units (IMUs) are placed on the arm and forearm of the exoskeleton. In addition to providing linear acceleration ($\ddot{x}_{imu}$) and angular velocity ($\dot{q}_{imu}$), the IMUs' orientation (q_{imu}) is estimated using an embedded Kalman filter. A strain gauge is mounted between the exoskeleton forearm and the forearm cuff, and calibrated to measure interaction forces (F_m). All sensors and the microcontroller are connected to a USB hub that communicates with a remote computer.

The microcontroller (low-level control) uses Field-Oriented Control (FOC) to drive the motor in torque mode, according to the torque reference (τ_{cmd}) provided by the remote computer (high-level control, see Section II-C). FOC is done using the SimpleFOC Arduino library [25]. The torque-to-current calibration is done statically, and additional damping is applied in the control loop to increase stability. The low-level control loop runs at 1 kHz and communicates with the computer at 110 Hz through Serial. The overall control architecture of the exoskeleton is displayed in Fig. 2.

B. Motion Prediction

When motion prediction is used in the exoskeleton control, the computation of the reference elbow torque τ_{cmd} in the high-level control is based on the predicted angular position q_p^{elb} of the exoskeleton elbow joint. In this work, given that we focus on a 1 DoF movement, we use a light-weight MLP network for the prediction [18]. The MLP is trained to approximate the function f, predicting the future value of the exoskeleton elbow position q^{elb} at a prediction horizon t_p based on the time-series history t_h of q^{elb} (*Seq to one* paradigm):

$$f(q^{elb}_{t-t_h \to t}) = q^{elb}_{t+t_p} = q^{elb}_p. \quad (1)$$

We use a simple MLP architecture containing 2 layers of 32 neurons (the parameters of the network architecture were hand-tuned to minimize its size for a sufficient prediction performance). In this work, we empirically selected a past window t_h of 500 ms and a prediction horizon t_p of 120 ms. The MLP is trained using supervised learning on data from a pilot experiment (see Section III-C).

C. Exoskeleton Control

This study aims to evaluate the effect of motion prediction on transparency. Hence, we compare the performance of predictive controllers (τ_{cmd} is computed using the exoskeleton predicted angular position q_p^{elb}) with standard (non-predictive) controllers. Since we focus on transparency, the goal of the exoskeleton motor torque is only to compensate for the effects due to the exoskeleton structure (there is no external load compensation, nor does the exoskeleton support part of the user's arm weight). We compare a baseline condition where the exoskeleton motor is turned off, two standard controllers from the literature [26] [27], and a predictive version of these two controllers. The different controllers are described hereafter and summarized in Fig. 2:

[1]This prototype has been designed specifically for a transparency study, and not for load manipulation, hence the limited actuation power.

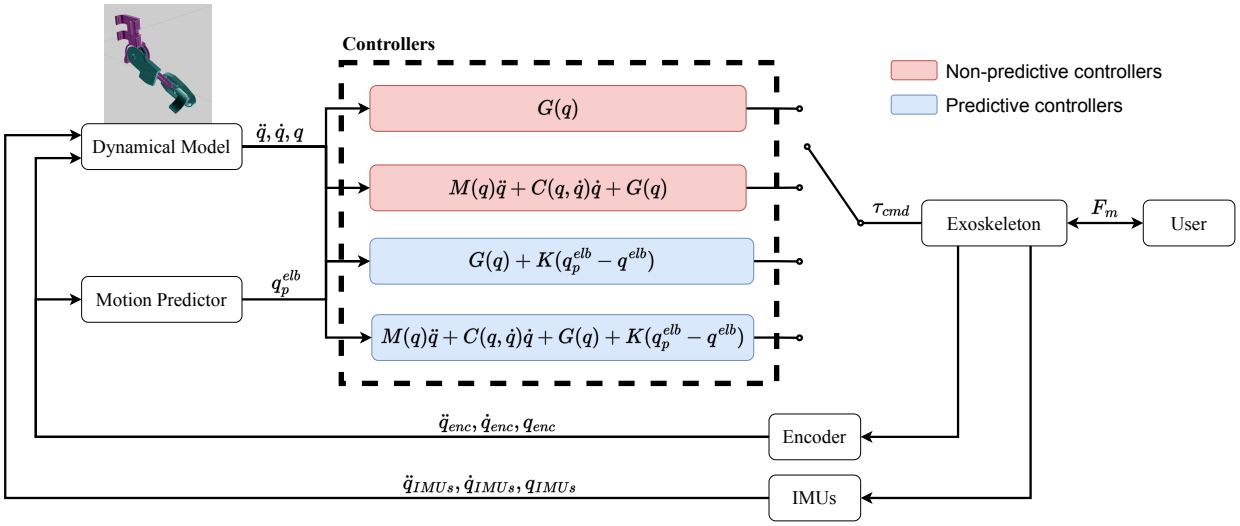

Fig. 2: Control scheme of the exoskeleton. q is the vector of generalized coordinates of the exoskeleton and $\dot{q}$ and $\ddot{q}$ are the corresponding velocity and acceleration

1) Exoskeleton off (O): The motor is turned off. Thanks to the direct-drive actuation, the exoskeleton is backdrivable and can easily be moved even when unpowered.

2) Gravity compensation (G): The exoskeleton torque compensates for the gravity effects of the exoskeleton structure according to[2]:

$$\tau_{cmd} = G(q) \tag{2}$$

with q the generalized coordinates of the exoskeleton (elbow angular position and upper-arm Cartesian orientation), and G the vector of gravity effects.

3) Dynamic compensation (D): The exoskeleton torque compensates for the full dynamics of the exoskeleton structure according to dynamic model equation:

$$\tau_{cmd} = M(q)\ddot{q} + C(q,\dot{q})\dot{q} + G(q) \tag{3}$$

with $\dot{q}$ and $\ddot{q}$ the exoskeleton velocity and acceleration respectively, estimated from numerical derivation (Section II-A), M the inertia matrix, and C the vector of Coriolis and centrifugal effects.

4) Gravity compensation with Prediction (GP): This controller expands the gravity compensation controller by adding a predictive correction, in order to help compensate for ill-modeled effects. The correction is defined as a proportional control between the predicted position q_p^{elb} and the current position q^{elb} of the elbow joint:

$$\tau_{cmd} = G(q) + K(q_p^{elb} - q^{elb}) \tag{4}$$

with K the gain of the correction.

5) Dynamic compensation with Prediction (DP): This controller expands the dynamic compensation controller by adding the same predictive correction as in GP:

$$\tau_{cmd} = M(q)\ddot{q} + C(q,\dot{q})\dot{q} + G(q) + K(q_p^{elb} - q^{elb}). \tag{5}$$

[2]In the remaining of the paper, τ_{cmd} actually corresponds only to the elbow component of the gravity (resp. dynamic) model equation. We omit the component notation in the equations for the sake of simplicity.

The online computation of the exoskeleton dynamic model is done with the Pinocchio library [28]. The value of K in the predictive controllers is experimentally tuned to 0.3 N.m.

III. Experiment

We conducted a user study to compare the effect on transparency of the 4 controllers and the baseline described in the previous section. Participants performed a virtual pointing task, common in exoskeleton studies [29], and both objective and subjective metrics for transparency were assessed. The experiment is described hereafter.

A. Participants

15 volunteers participated in the experiment (9 men and 6 female; 13 right-handed and 2 left-handed; age: 26.7 ± 2.4 yo; height: 1.71 ± 0.10 m; mass: 68.1 ± 13.7 kg). Participants were recruited from a convenience sample of lab members with no exoskeleton experience. They declared no musculoskeletal or neurological disorder in the upper limb in the past months. All participants signed an informed consent form before participating in the experiment. The experiment was approved by the Ethics Committee of Inria (COERLE) and was conducted in accordance with the Declaration of Helsinki.

B. Experimental Setup

1) Experimental Task: Participants were instructed to perform a virtual pointing task with their left arm, consisting in moving a cursor on a screen placed in front of them (Fig. 1). The vertical position of the cursor was controlled by the angular position of the exoskeleton elbow joint. One trial consisted in moving the cursor (displayed as a blue circle) from a fixed initial position at the bottom of the screen to a target position (displayed as a red circle), keeping the cursor on the target during 100 ms with a tolerance of 1 deg, then moving the cursor back to the initial position (second target). The initial position corresponded to a position where the elbow

was fully extended. The heights of the targets were scaled for each participant, depending on their maximum (comfortable) voluntary elbow flexion when wearing the exoskeleton. The average range of motion from initial position to target across participants was 65 deg for the lowest target, and 115 deg for the highest target.

2) Experimental design: One condition (*i.e.* one controller) consisted of 25 successive trials (no break between trials), with 5 different target heights (5 trials for each height) performed in random order. Each condition started with a familiarization phase of 3 trials (in addition to the 25 test trials). The 5 conditions were performed in random order, with a 2 min break (approximately) between each condition.

C. Motion Predictor Training

A dataset was collected to train the MLP model on the pointing task. Four participants (different from the participants in the main experiment) performed a pilot experiment without the predictive controllers. They performed 49 trials (7 trials for 7 target heights) with each of the 3 non-predictive conditions (exoskeleton off, gravity compensation and dynamics compensation). This dataset of 588 trials was separated into a training set (70 %), a validation set (15 %) and a testing set (15 %). For both the training and the online prediction, angular position data were downsampled to 25 Hz in order to reduce the size of the input data (deemed sufficient given the dynamics of the considered human motions). The Mean Squared Error (MSE) loss was used for training.

D. Performance Metrics

1) Task Performance: Task performance was assessed in each trial with two metrics: the duration of the trial (from appearance of the target to stabilized return to the start position), and the maximum size of the overshoot.

2) Interaction Force: In this experiment, the goal of the exoskeleton was not to provide a specific assistance to the user, but to be as transparent as possible, i.e. minimize the interaction force. Hence we quantified transparency using the measured human-exoskeleton interaction force, with two metrics: the root mean square (RMS) value of the interaction force over a trial, and the maximum absolute value of the interaction force within a trial. To facilitate between-subject comparison and because different participants exhibited different baseline force, the RMS force value was normalized according to its minimum and maximum values across all trials of all conditions of a participant.

3) Movement Smoothness: Natural human movements are known to be smooth. Therefore the smoothness of a motion is a relevant feature to evaluate if the interaction with an exoskeleton perturbs the human motion [30]. We used the Spectral Arc length (SPARC) metrics [31] to quantify movement smoothness of each trial in a way that is robust to variations in trial duration.

4) Subjective Evaluation: After each condition, participants were asked to rank how they liked this condition (controller) with respect to the previous ones. This ended up in a final ranking, with possible ex-aequo between conditions.

5) Prediction Performance: In addition to the previous metrics that focus on the human interaction with the exoskeleton, we also evaluated the prediction performance of the trained MLP model. Prediction performance was assessed using the RMSE value and the maximum error value between the predicted elbow angular position and the ground truth recorded with the encoder. We evaluated both the offline performance after training (i.e. using the testing dataset of the pilot experiment), and the online performance (i.e. using the data from the actual participants). For the offline performance, we computed one single RMSE over the whole training set (corresponding to the loss function used when training the model). For the online performance, we computed an RMSE (resp. maximum error) for each trial and both predictive controllers. We compared the performance of our MLP predictor with two baselines from the literature: a constant predictor (i.e. $q^{elb}_{t+t_p} = q^{elb}_t$) [18], and a constant velocity predictor (i.e. $q^{elb}_{t+t_p} = q^{elb}_t + \dot{q}^{elb}_t t_p$) [32].

E. Data Analysis

For each objective metrics, we computed its average value across all trials of a participant in a given condition in order to obtain one single value per participant and condition. The following analyses were conducted on these average values. Numerical data (task duration, RMS and maximum value of interaction force, and spectral arc length) were tested for normality using the Shapiro-Wilk test. All data were normally distributed. A one-way repeated measures ANOVA was then performed on each numerical metrics, with *participant* as a random factor and *condition* as a fixed factor. When a significant effect of *condition* was detected by the ANOVA, post-hoc multiple comparisons with Bonferroni correction were conducted. The ranking of the different controllers (subjective evaluation) was considered as categorical data, and was analyzed with a non-parametric Friedman test. A significance level of 5 % was adopted for all statistical tests, and analyses were performed in Python.

IV. Results

A. Task Performance

The ANOVA did not reveal any significant effect of the controller factor on either the trial duration ($F(4, 56) = 1.7$, $p = .16$) or the overshoot ($F(4, 56) = 1.9$, $p = .12$). The average duration of a trial across all targets, all conditions and all participants was 3.53 ± 0.83 s. The average overshoot of a trial across all targets, all conditions and all participants was 1.45 ± 0.62 deg.

B. Interaction Force

Fig. 3 depicts the time-evolution of the interaction force of a representative subject for the 5 different controllers. When the exoskeleton is off (O), the interaction force is always positive (i.e. in the direction of elbow extension, due to the exoskeleton weight), and significantly larger than in any of the 4 other conditions. In the 4 compensatory conditions (G, D, GP, DP), the interaction force oscillates around zero, with smaller peaks when the controller relies on motion prediction (GP, DP).

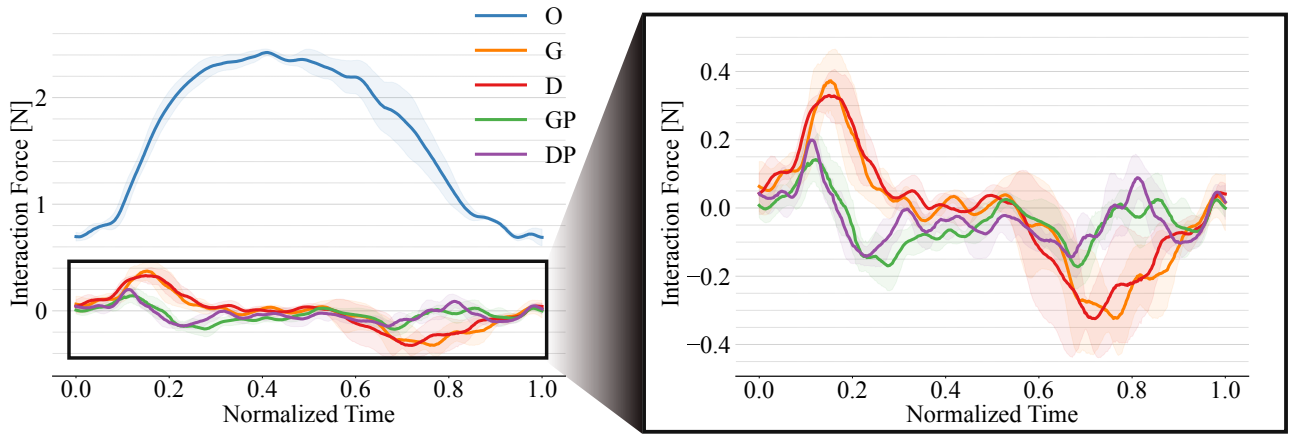

Fig. 3: Normalized time-evolution of the human-exoskeleton interaction force of a representative participant for the 5 controllers (O: Exoskeleton off, G: Gravity compensation, D: Dynamics compensation, GP: Gravity compensation with prediction, DP: Dynamics compensation with prediction). Force is positive in the direction of elbow extension. Only one target among the five target heights experienced by the participant is displayed. The graph shows both the upward and consecutive downward movement. For each controller, bold line (resp. shaded area) represents the mean (resp. standard deviation) over the 5 trials performed by the participant. The graph on the right side is a zoomed view.

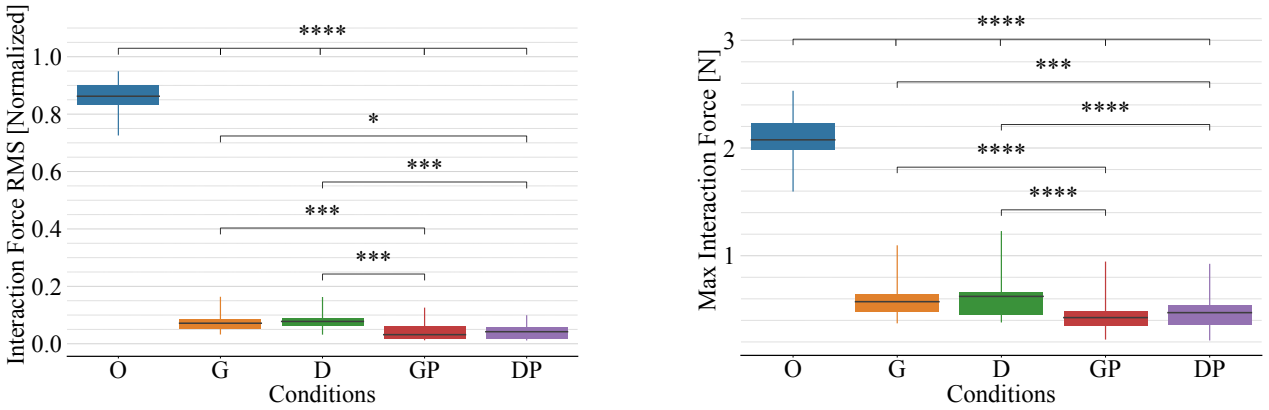

(a) Distribution of the normalized RMS value of the human-exoskeleton interaction

(b) Distribution of the peak value of the human-exoskeleton interaction force

Fig. 4: Distributions of human-exoskeleton interaction force metrics across all trials and all participants, for the 5 conditions (O: Exoskeleton off, G: Gravity compensation, D: Dynamics compensation, GP: Gravity compensation with prediction, DP: Dynamics compensation with prediction). Black lines represent the median. Stars indicate significant differences between the conditions.

Fig. 4 displays the distribution of the normalized RMS force value (4a) and of the peak interaction force (4b), for the 5 controllers. The ANOVA revealed a significant effect of the controller on both the normalized RMS force ($F(4, 56) = 1293.9$, $p < .0001$)), and the peak force ($F(4, 56) = 326.6$, $p < .0001$). Post-hoc pairwise comparisons revealed that both the RMS force and the peak force in the Exoskeleton Off (O) condition differed significantly from the 4 other conditions ($p < .0001$). The two predictive controllers (GP and DP) differed significantly from the two non-predictive controllers (G and D) for both metrics (RMS force: G-GP: $p = .0002$, D-DP: $p = .0004$, G-DP: $p = .015$, D-GP: $p = .0003$; Peak force: G-GP: $p < .0001$, D-DP: $p = .0001$, G-DP: $p = .0004$, D-GP: $p < .0001$). Adding prediction to the controller lead to an average reduction in RMS force (resp. peak force) of 39 % (resp. 26 %) for gravity compensation, and of 45 % (resp. 27 %) for dynamics compensation. However there was no significant difference between gravity compensation and dynamics compensation for any of the two force metrics, whether prediction was used or not ($p = 1.0$ for both metrics and both G-D and GP-DP comparisons).

C. Movement Smoothness

Fig. 5 depicts the time-evolution of the elbow angular velocity of a representative subject for the 5 different controllers.

The velocity profiles are overall similar for all controllers, though the velocity peak seems slightly different for the non-predictive controllers in the downward movement. The ANOVA did not reveal any significant effect of the controllers on the SPARC metrics ($F(4, 56) = 2.0, p = .11$). The average value of the SPARC metrics in a trial across all targets, all conditions and all participants was -1.68 ± 0.32.

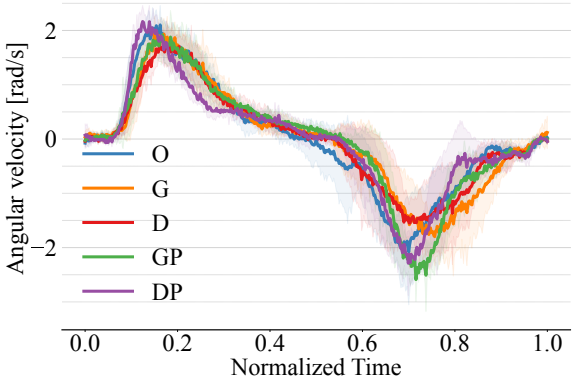

Fig. 5: Normalized time-evolution of the elbow angular velocity of a representative participant for the 5 controllers (O: Exoskeleton off, G: Gravity compensation, D: Dynamics compensation, GP: Gravity compensation with prediction, DP: Dynamics compensation with prediction). Only one target among the five target heights experienced by the participant is displayed. The graph shows both the upward and consecutive downward movement. For each controller, bold line (resp. shaded area) represents the mean (resp. standard deviation) over the 5 trials performed by the participant.

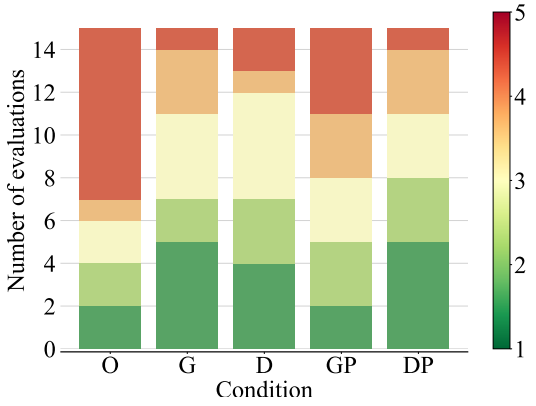

Fig. 6: Subjective ranking of the 5 controllers performed by participants (O: Exoskeleton off, G: Gravity compensation, D: Dynamics compensation, GP: Gravity compensation with prediction, DP: Dynamics compensation with prediction). The Y-axis displays the number of times a controller was ranked at any position between 1 (most preferred, green) and 5 (least preferred, red).

TABLE I: Maximum error and RMSE between predicted and measured elbow angular position in degrees average for every trial and every participant for each predictive condition and predictors.

		GP	DP
Constant Position Predictor	Max	11.7 ± 3.27	12.03 ± 3.28
	RMSE	5.73 ± 1.37	5.75 ± 1.46
Constant Velocity Predictor	Max	6.34 ± 2.1	6.34 ± 2.1
	RMSE	1.73 ± 0.47	1.74 ± 0.48
MLP	Max	**4.67** ± 1.69	4.78 ± 1.83
	RMSE	**1.43** ± 0.39	1.45 ± 0.39

D. Subjective Evaluation

Fig. 6 displays the ranking of the 5 controllers across all participants. While the Exoskeleton Off (O) condition was ranked least preferred more times than any of the 4 other conditions, the Friedman ANOVA did not reveal any significant effect of the controller factor on the ranking ($\chi^2(4) = 6.47, p = .17$).

E. Prediction Performance

The offline test RMSE (test loss) between predicted values and ground truth was $6.0\,deg$ for the constant position predictor and $1.1\,deg$ for our MLP. Table I shows the results of the online evaluation of the predictions. There are few differences between the GP and DP controllers. Both the constant velocity and MLP predictors yield far superior results compared to the constant position predictor. While the constant velocity and MLP predictors have similar performance in terms of RMSE, the maximum error is lower by 35% on average with the MLP predictor.

V. Discussion

This study introduced motion prediction based on kinematic data from embedded sensors for the control of an active upper-limb exoskeleton and investigated whether such predictive control is beneficial for transparency. The impact of prediction was assessed both for gravity-compensation and for dynamics-compensation. Results show that prediction reduced interaction force without affecting the kinematics of the movement, even though it was not perceived by users.

A. Gravity vs. Dynamics Compensation

We did not observe any difference between a gravity-compensation control and a dynamics-compensation control on either the kinematics of the movement, the interaction force, or the user perception of transparency. This absence of difference was present both without and with prediction. Conversely to our results, Verdel *et al.* reported an increase in movement duration of a pointing task when only gravity and friction were compensated, as opposed to full dynamics compensation [27]. However, the exoskeleton used in their study was heavier than ours. The light weight of our exoskeleton associated with the limited speed of motion likely result in negligible inertial effects, explaining the similarity between the gravity- and dynamics-compensation control.

B. Effect of Prediction on Transparency

The kinematics of the pointing motion (movement duration, smoothness, and overshoot) were not modified by the

predictive controllers, compared both to non-predictive controllers and to the baseline condition where the exoskeleton was turned off. While we cannot guarantee that the kinematic properties of the natural human movement (i.e. without exoskeleton) were preserved with the exoskeleton, elements from the literature suggest so. Actually, Verdel *et al.* showed that in a similar pointing task, natural movement duration was preserved with an exoskeleton if the full dynamics was compensated [27]. Thus adding prediction in the controller did not perturb the intrinsic features of the human motion.

Regarding human-exoskeleton interaction force, predictive controllers lead to a force reduction compared to non-predictive controllers, which suggests improved transparency. According to the force profiles in Fig. 3, without prediction the user is always pushing against the exoskeleton (positive force in the flexion motion, and negative force in the extension motion). This means that the user has to (slightly) force against the exoskeleton to make it move. This effect might explain why the velocity peak is slightly smaller with the non-predictive controllers (Fig. 5). Conversely, when prediction is used, the force peaks are smaller and in the direction of motion[3], meaning that the exoskeleton facilitates the user's movement. From a physical standpoint, the magnitude of the force reduction is limited (about $0.2\,\mathrm{N}$). However our exoskeleton is mechanically very transparent, owing to its light weight and direct-drive actuation without reduction, so forces at play are always small. Actually, these results demonstrate that even with an exoskeleton that is transparent by design, motion prediction can further increase the transparency. Hence we could expect prediction to be even more beneficial with a heavier or less backdrivable exoskeleton.

Despite the force reduction associated with prediction, users did not rank the predictive controllers any differently from the other conditions. This may be due to the low forces at play, making it difficult for users to discriminate between the different conditions due to sensory limitations (made even harder by the motion and the fact that is was not a primary objective). Moreover, the transparency concept was not trivial for many participants who sometimes mixed perceived assistance and transparency.

C. Prediction Performance

The MLP model used in this work was a light network, yet it yielded better results than both constant position and constant velocity predictor baselines. Specifically, the maximum error was reduced with the MLP, which is advisable both for users' safety and comfort. We evaluated both the online and offline performance of our MLP predictor. Yet, online results should be considered carefully as the predicted motion is used in the exoskeleton control, which may affect the human motion, possibly resulting in an actual motion continuation different from the one planned by the user. However, the low interaction forces at play and the similar movement kinematics with vs. without prediction suggest that the exoskeleton did not significantly perturb the motion. This is consistent with the fact that online and offline prediction errors were similar.

Interestingly, predictive and non-predictive controllers exhibited similar behaviors in the early stage of the motion, with an increase in interaction force resisting the movement (Fig. 3, 0–10 % and 55–65% of movement time approximately). Then the magnitude of the force rapidly decreases when prediction is used. This suggests that prediction is not accurate in the early moments following movement initiation. The model can hardly predict future motion from an immobile state and needs a sufficient history of actual movement to make an accurate prediction.

A limitation of this study is that the experimental task requires only simple pointing movements, hence the challenge of motion prediction is limited. This explains why using a simple MLP predictor was sufficient. While using motion prediction in the exoskeleton control was shown beneficial for transparency, this highly depends on the quality of the prediction. More complex 3D arm motions may be harder to accurately predict, and would probably require a more complex neural network architecture, such as RNN or diffusion-based architectures. In the future, we will extend our motion prediction approach to such more complex movements, yet trying to keep a relatively lightweight architecture for the predictor. Indeed, we target industrial tasks that, while more varied than simple pointing tasks, remain limited in their diversity. In an industrial context, limiting the amount of data required to train the predictor is a crucial point. Moreover, these predictors should be embedded on microcontrollers with limited computational power for online usage, making it even more important to keep them as light as possible.

Finally, several parameters of the predictor were manually tuned (e.g., gain K, prediction horizon t_h). In future work, we plan to optimize their value to provide personalized assistance –for instance, using Human in the Loop Optimization (HIL) [33]–, or adapt them depending on the context or the prediction uncertainty.

VI. Conclusion

This work introduced a motion prediction-based control approach for an active upper-limb exoskeleton, using an MLP model to predict the human arm motion from sensor data embedded on the exoskeleton. We then investigated whether such a predictive controller improves the exoskeleton transparency. A user study was conducted in which participants performed a pointing task with the exoskeleton, controlled either with predictive controllers or with standard non-predictive controllers. The predictive controllers reduced the human-exoskeleton interaction force by about 40 % compared to non-predictive controllers, without affecting the kinematics of the human motion. However, the participants did not perceive a noticeable difference in transparency between the different conditions. This was probably due to the fact that the exoskeleton used in the study was mechanically very transparent, hence the forces at play were small in all conditions. Nevertheless, these results suggest that motion prediction-based control can

[3]Leaving aside the first force peak immediately following movement initiation, which corresponds to when prediction is not yet useful, see Section V-C

further improve transparency, even on an exoskeleton that is already transparent by design.

In future work, we will test the effect of motion prediction-based control on more complex motions, where prediction will be further challenged. We will then transfer the predictive control approach to an exoskeleton designed for assistance of load handling (a few kg). Such assistance requires a more powerful exoskeleton, hence heavier and less backdrivable since reduction will be needed in the actuation. We expect predictive controllers to be even more beneficial since the exoskeleton will be mechanically less transparent and higher interaction forces will then be at play.

VII. Ackowledgments

This research was supported by the CPER CyberEntreprises, the Creativ'Lab platform of Inria/LORIA, the EU Horizon project euROBIN (GA n.101070596), the France 2030 program through project PEPR O2R AS3 and PI3 (ANR-22-EXOD-007, ANR-22-EXOD-004).The authors would like to thank R. Lartot and R. Bousigues for their help with designing the prototype exoskeleton.

References

[1] de Kok, Jan and Vroonhof, Paul and Snijders, Jacqueline and Roullis, Georgios and Clarke, Martin and Peereboom, Kees and van Dorst, Pim and Isusi, Iñigo, *Work-related Musculoskeletal Disorders: prevalence, costs and demographics in the EU*. Publications Office, 2019.

[2] J. Theurel and K. Desbrosses, "Occupational exoskeletons: overview of their benefits and limitations in preventing work-related musculoskeletal disorders," *IISE Transactions on Occupational Ergonomics and Human Factors*, 2019.

[3] T. Moeller, J. Krell-Roesch, A. Woll, and T. Stein, "Effects of upper-limb exoskeletons designed for use in the working environment—a literature review," *Frontiers in Robotics and AI*, 2022.

[4] S. Toxiri, M. B. Näf, M. Lazzaroni, J. Fernández, M. Sposito, T. Poliero, L. Monica, S. Anastasi, D. G. Caldwell, and J. Ortiz, "Back-support exoskeletons for occupational use: an overview of technological advances and trends," *IISE Transactions on Occupational Ergonomics and Human Factors*, 2019.

[5] T. Poliero, V. Fanti, M. Sposito, D. G. Caldwell, and C. Di Natali, "Active and passive back-support exoskeletons: a comparison in static and dynamic tasks," *IEEE Robotics and Automation Letters*, 2022.

[6] J. Riemer and S. Wischniewski, "Long-term effects and user acceptance of back-support exoskeletons in the workplace," *Zeitschrift für Arbeitswissenschaft*, 2023.

[7] S. Luo, M. Jiang, S. Zhang, J. Zhu, S. Yu, I. Dominguez Silva, T. Wang, E. Rouse, B. Zhou, H. Yuk, X. Zhou, and H. Su, "Experiment-free exoskeleton assistance via learning in simulation," *Nature*, 2024.

[8] P. Malcolm, W. Derave, S. Galle, and D. D. Clercq, "A Simple Exoskeleton That Assists Plantarflexion Can Reduce the Metabolic Cost of Human Walking," *PLOS ONE*, 2013, publisher: Public Library of Science.

[9] M. Kim, Y. Ding, P. Malcolm, J. Speeckaert, C. J. Siviy, C. J. Walsh, and S. Kuindersma, "Human-in-the-loop Bayesian optimization of wearable device parameters," *PLOS ONE*, 2017.

[10] P. Sedighi, X. Li, and M. Tavakoli, "EMG-Based Intention Detection Using Deep Learning for Shared Control in Upper-Limb Assistive Exoskeletons," *IEEE Robotics and Automation Letters*, 2023.

[11] J. C. Gillette and M. L. Stephenson, "Electromyographic Assessment of a Shoulder Support Exoskeleton During on-Site Job Tasks," *IISE Transactions on Occupational Ergonomics and Human Factors*, 2019.

[12] C. Piozin, G. H. Altamira, C. Simon, B. Lavrard, J.-Y. Audran, F. Waszak, and S. Eskiizmirliler, "Motion prediction for the sensorimotor control of hand prostheses with a brain-machine interface using EEG," in *2022 10th International Winter Conference on Brain-Computer Interface (BCI)*, 2022.

[13] M. Gulzar, Y. Muhammad, and N. Muhammad, "A Survey on Motion Prediction of Pedestrians and Vehicles for Autonomous Driving," *IEEE Access*, 2021.

[14] S. S. Ge, Y. Li, and H. He, "Neural-network-based human intention estimation for physical human-robot interaction," in *2011 8th International Conference on Ubiquitous Robots and Ambient Intelligence (URAI)*, 2011.

[15] J. N. Kundu, M. Gor, and R. V. Babu, "BiHMP-GAN: Bidirectional 3D Human Motion Prediction GAN," *Proceedings of the AAAI Conference on Artificial Intelligence*, 2019.

[16] K. Fragkiadaki, S. Levine, P. Felsen, and J. Malik, "Recurrent Network Models for Human Dynamics," in *2015 IEEE International Conference on Computer Vision (ICCV)*. Santiago, Chile: IEEE, 2015.

[17] G. Tevet, S. Raab, B. Gordon, Y. Shafir, A. H. Bermano, and D. Cohen-Or, "Human Motion Diffusion Model," 2022.

[18] W. Guo, Y. Du, X. Shen, V. Lepetit, X. Alameda-Pineda, and F. Moreno-Noguer, "Back to MLP: A Simple Baseline for Human Motion Prediction," 2022.

[19] M. Jamšek, T. Kunavar, U. Bobek, E. Rueckert, and J. Babič, "Predictive Exoskeleton Control for Arm-Motion Augmentation Based on Probabilistic Movement Primitives Combined With a Flow Controller," *IEEE Robotics and Automation Letters*, 2021.

[20] F. Lanotte, Z. McKinney, L. Grazi, B. Chen, S. Crea, and N. Vitiello, "Adaptive Control Method for Dynamic Synchronization of Wearable Robotic Assistance to Discrete Movements: Validation for Use Case of Lifting Tasks," *IEEE Transactions on Robotics*, 2021.

[21] A. O. Souza, J. Grenier, F. Charpillet, P. Maurice, and S. Ivaldi, "Towards data-driven predictive control of active upper-body exoskeletons for load carrying," in *2023 IEEE International Conference on Advanced Robotics and Its Social Impacts (ARSO)*. IEEE, 2023.

[22] D. Verdel, G. Sahm, S. Bastide, O. Bruneau, B. Berret, and N. Vignais, "Influence of the Physical Interface on the Quality of Human–Exoskeleton Interaction," *IEEE Transactions on Human-Machine Systems*, 2023.

[23] S. Dalla Gasperina, A. L. Ratschat, and L. Marchal-Crespo, "Quantitative and qualitative evaluation of exoskeleton transparency controllers for upper-limb neurorehabilitation," in *2023 International Conference on Rehabilitation Robotics (ICORR)*. IEEE, 2023.

[24] N. Jarrasse, J. Paik, V. Pasqui, and G. Morel, "How can human motion prediction increase transparency?" in *2008 IEEE International Conference on Robotics and Automation*, 2008.

[25] A. Skuric, H. Bank, R. Unger, O. Williams, and D. González-Reyes, "SimpleFOC: A Field Oriented Control (FOC) Library for Controlling Brushless Direct Current (BLDC) and Stepper Motors," *Journal of Open Source Software*, vol. 7, p. 4232, Jun. 2022.

[26] S. Bastide, N. Vignais, F. Geffard, and B. Berret, "Interacting with a "Transparent" Upper-Limb Exoskeleton: A Human Motor Control Approach," in *2018 IEEE/RSJ International Conference on Intelligent Robots and Systems (IROS)*. Madrid: IEEE, 2018.

[27] D. Verdel, S. Bastide, N. Vignais, O. Bruneau, and B. Berret, "An Identification-Based Method Improving the Transparency of a Robotic Upper Limb Exoskeleton," *Robotica*, 2021.

[28] J. Carpentier, G. Saurel, G. Buondonno, J. Mirabel, F. Lamiraux, O. Stasse, and N. Mansard, "The Pinocchio C++ library : A fast and flexible implementation of rigid body dynamics algorithms and their analytical derivatives," in *2019 IEEE/SICE International Symposium on System Integration (SII)*, 2019.

[29] S. Bastide, N. Vignais, F. Geffard, and B. Berret, "Interacting with a "Transparent" Upper-Limb Exoskeleton: A Human Motor Control Approach," in *2018 IEEE/RSJ International Conference on Intelligent Robots and Systems (IROS)*. Madrid: IEEE, Oct. 2018, pp. 4661–4666. [Online]. Available: https://ieeexplore.ieee.org/document/8593991/

[30] R. O. Hailey, A. C. De Oliveira, K. Ghonasgi, B. Whitford, R. K. Lee, C. G. Rose, and A. D. Deshpande, "Impact of Gravity Compensation on Upper Extremity Movements in Harmony Exoskeleton," in *2022 International Conference on Rehabilitation Robotics (ICORR)*. Rotterdam, Netherlands: IEEE, Jul. 2022, pp. 1–6. [Online]. Available: https://ieeexplore.ieee.org/document/9896415/

[31] S. Balasubramanian, A. Melendez-Calderon, A. Roby-Brami, and E. Burdet, "On the analysis of movement smoothness," *Journal of NeuroEngineering and Rehabilitation*, 2015.

[32] C. Schöller, V. Aravantinos, F. Lay, and A. C. Knoll, "The simpler the better: Constant velocity for pedestrian motion prediction," *CoRR*, 2019.

[33] P. Slade, M. J. Kochenderfer, S. L. Delp, and S. H. Collins, "Personalizing exoskeleton assistance while walking in the real world," *Nature*, 2022.